

Geometry-Dependent Si(2*p*) Surface Core-Level Excitations for Si(111) and Si(100) Surfaces

F. J. Himpsel, P. Heimann, T.-C. Chiang, and D. E. Eastman

IBM Thomas J. Watson Research Center, Yorktown Heights, New York 10598

(Received 27 June 1980)

Structure-dependent Si(2*p*) surface core-level shifts and 2*p* photothreshold spectra which yield new surface geometry information are reported. For Si(100)-(2×1), ~0.5 mono-layer of surface atoms are found shifted to smaller binding energy (-0.5 eV) relative to the bulk; this rules out symmetric pairing models. Si(111)-(7×7) and Si(111)-(2×1) show different surface 2*p* core-level spectra (e.g., $\frac{1}{4}$ layer shifted -0.7 eV versus $\frac{1}{2}$ layer shifted -0.4 eV), suggesting different geometries. Si(111)-(1×1)H exhibits first-layer (+0.26 eV) and second-layer (+0.15 eV) shifts.

PACS numbers: 68.20.+t, 79.60.Eq

Angle-integrated (~1.8 sr) photoelectron spectra were taken with a display-type spectrometer⁸ with use of synchrotron radiation from the 240-MeV Tantalus-I storage ring. The Si(111)-(2×1) surface was prepared by cleaving in vacuum (mid-10⁻¹¹-Torr range); single domain cleaves were selected with no visible streaking of the LEED pattern (i.e., few steps). Exposing this surface to activated hydrogen resulted in a Si(111)-(1×1)H surface. The Si(100)-(2×1) and Si(111)-(7×7) surfaces were prepared by very mild sputtering and by heating off the oxide film. Nearly intrinsic wafers were used ($\approx 10 \Omega \text{ cm}$ with large Debye screening lengths) with different dopings (*p*-type boron doped and *n*-type phosphor doped) to rule out band-bending effects. Fermi-level reference energies were obtained by measuring the Fermi edge of the Ta sample holder.

Si(2*p*) core-level angle-integrated photoemission spectra for Si(100)-(2×1) are shown in Fig. 1 for two photon energies, $h\nu = 108$ and 130 eV. For $h\nu = 130$ eV, a shoulder is observed on the low-binding-energy side of the spin-orbit-split $2p_{1/2,3/2}$ doublet. This shoulder is very weak for $h\nu = 108$ eV where the escape depth of the 2*p* photoelectrons is much longer than at the higher energy (final energy of ≈ 9 eV above E_F vs 31 eV). Exposure of this surface to oxygen or hydrogen quenches this surface-state level and introduces chemically shifted surface core levels on the high-binding-energy side of the bulk peak (not shown in Fig. 1). This rules out monochromator and spectrometer artifacts.

We have decomposed the spectra in Fig. 1 into similarly shaped $2p_{1/2}$ and $2p_{3/2}$ contributions (as shown by dashed lines) and have analyzed Si bulk and surface core-level features using a least squares fitting program with Lorentzian line shapes of equal width. From this, a spin-orbit

splitting of $\Delta = 0.61 \pm 0.01$ eV was determined with a ($p_{1/2}/p_{3/2}$) branching ratio R that varied from 0.51 at $h\nu = 108$ eV to 0.53 at $h\nu = 130$ eV which is close to the statistical ratio of $R = 0.5$. This suggests that diffraction effects⁹ are small.

Spin-orbit-decomposed $2p_{3/2}$ spectra for all Si surfaces studied are shown in Fig. 2 (solid lines). Together with surface-sensitive spectra at $h\nu = 120$ eV, we show one bulklike spectrum ($h\nu = 108$ eV) for the hydrogen-terminated Si(111) surface. All energy scales have been referenced to the bulk Si $2p_{3/2}$ core-level position as measured for $h\nu \approx 108$ eV. Using our $2p_{3/2}$ binding energies measured relative to E_F and the value $E_F - E_v$

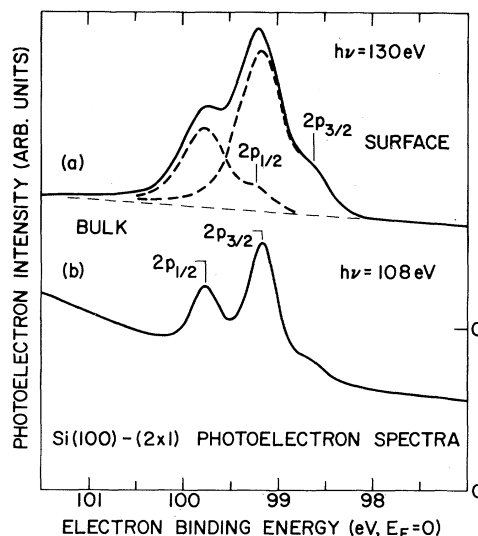


FIG. 1. Angle-integrated photoelectron spectra from Si(2*p*) levels for Si(100)-(2×1). Dashed lines depict decomposed $2p_{3/2}$ and $2p_{1/2}$ levels. Emission from surface 2*p* levels is seen on the low-binding-energy side of the bulk level for the surface-sensitive spectrum with $h\nu = 130$ eV.

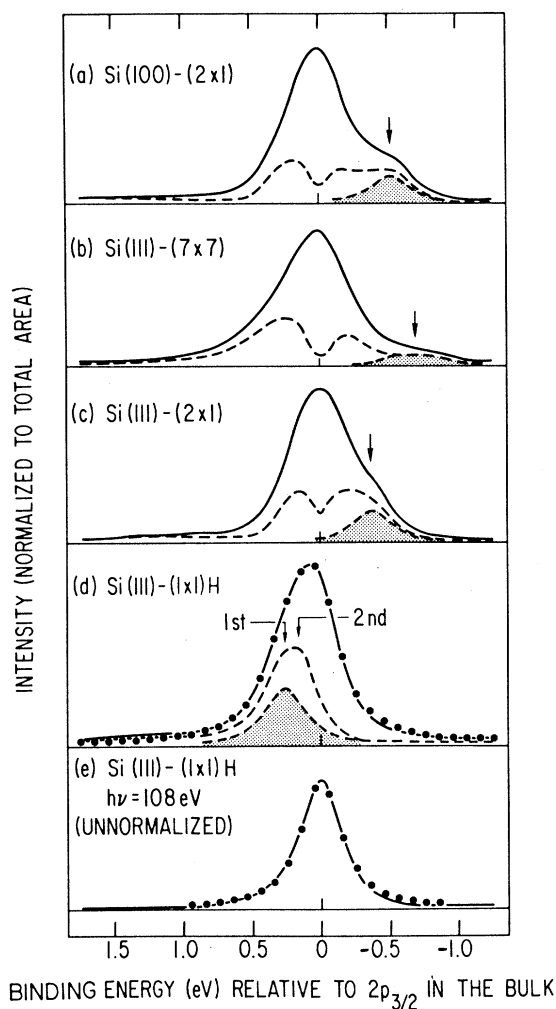


FIG. 2. $\text{Si}(2p_{3/2})$ core-level spectra for various surfaces (full lines). $h\nu = 120$ eV. The dashed lines (without crosshatching) show the contribution of the outer two surface layers, after subtraction of the Lorentzian bulk contribution [dotted curve in (e)] which was obtained via a three-Lorentzian fit [dotted curve in (d)] to $\text{Si}(111)-(1 \times 1)\text{H}$ data. Certain surface core levels are cross-hatched.

$= 0.33$ eV for $\text{Si}(111)-(2 \times 1)$ from Allen and Gobel,¹⁰ we obtain $E_F - E_v = 0.34$, 0.51 , and 0.46 eV for $\text{Si}(100)-(2 \times 1)$, $\text{Si}(111)-(7 \times 7)$, and $\text{Si}(111)-(1 \times 1)\text{H}$, respectively.

We have determined the absolute numbers of surface atoms with shifted core levels by using the $\text{Si}(111)-(1 \times 1)\text{H}$ data for calibration. This surface has a fairly well-established configuration with hydrogen atoms terminating the dangling bonds of the truncated bulk structure. By fitting the $\text{Si} + \text{H}$ spectrum in Fig. 2(d), we have found

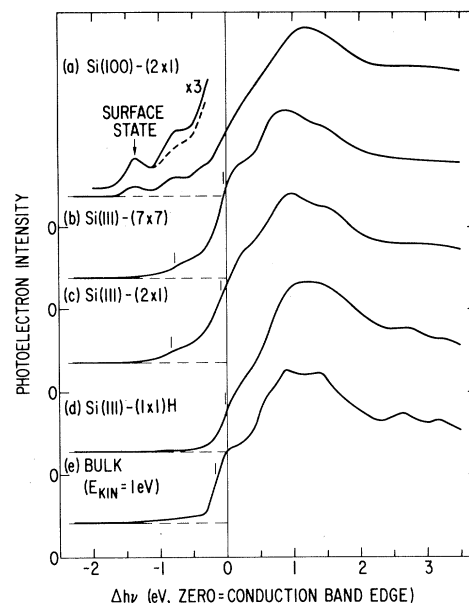


FIG. 3. Angle-integrated, CFS spectra for the $\text{Si } 2p$ edge. $E_{\text{kin}} = 80$ eV. Curves *a*–*d* represent surface-sensitive absorption-edge spectra while curve *e* represents the bulk absorption edge (see text). Ticmarks in curves *a*–*d* denote features involving surface $2p_{3/2}$ core-level transitions. The dashed line in curve *a* represents the $2p_{3/2}$ component of the spectrum. The energy zero corresponds to $h\nu = 99.97$ eV.

that two surface layer levels on the high-binding-energy side at $+0.26 \pm 0.02$ eV and $+0.16 \pm 0.02$ eV are required; we associate these with the first (outermost) H-terminated (111) surface layer (crosshatched line) and second surface layer (separated by only 0.78 Å), respectively. The bulk Lorentzian of this fit [shown by dots in Fig. 2(e)] is seen to describe the total $2p_{3/2}$ emission for $h\nu = 108$ eV [Fig. 2(e), full line] quite well. From the surface- to bulk-intensity ratio, we have determined a $2p$ -electron escape depth of 5.4 Å at $h\nu = 120$ eV, in agreement (within 1 Å) with other determinations.¹¹ The dashed lines without crosshatching in Fig. 2 show the contributions of the outer two surface layers after subtraction of a Lorentzian bulk contribution from the full lines in Fig. 2 (with an escape depth of 5.4 Å). Unlike $\text{Si}(111)-(1 \times 1)\text{H}$, the other surfaces involve more than two surface core levels. We have singled out several low-binding-energy surface levels by the Lorentzian-shaped dashed lines with hatching in Fig. 2. There is also at least one high-binding-energy level for all three clean surfaces [Figs. 2(a)–2(e)].

Before discussing the surface core-level fea-

tures in more detail, it is useful to describe the Si(2p) absorption-edge spectra for these same surfaces shown in Fig. 3. Curves *a-d* are surface-sensitive, constant-final-state (CFS) spectra taken with a kinetic energy of 80 eV and varying the photon energy $h\nu$. In analogy to Fig. 2, we also include a bulklike CFS spectra (1 eV kinetic energy, curve *e*) in Fig. 3. For curves *a-c*, features can be seen below the bulk 2p edge (*e*), while such features are missing for Si(111)-(1×1)H (curve *d*). These features correspond to transitions involving 2p surface core levels and/or empty surface states. In Fig. 3, the energy zero corresponds to the one-electron transition $2p_{3/2}$ → conduction-band edge in the bulk. The bulk Si(2p_{3/2}) edge (ticmark in Fig. 3, curve *e*) is shifted by excitonic effects.¹² The data in Figs. 2 and 3 have the following implications concerning various geometrical models for Si(100) and Si(111) surfaces.

Si(100)-(2×1).—This surface has been most widely described by use of a dimer or pairing model which is consistent with experimental surface-state band dispersions if an asymmetric buckling is included (asymmetric dimer model).^{1,7,13} The crosshatched surface core-level feature at -0.52 eV in Fig. 2(a) has an intensity which corresponds to one-half of a (100) layer; this feature is consistent with an asymmetric-dimer model and would be associated with the outwards shifted $\frac{1}{2}$ layer of surface (100) surface atoms. A symmetric-dimer model would have a full outer layer of shifted atoms, which is inconsistent with our data. A missing-row model³ is also consistent with our findings; the -0.52-eV core level would correspond to the ridge atoms. The surface CFS absorption-edge spectrum (Fig. 3 curve *a*), for Si(100)-(2×1) shows prominent transitions at -1.34 and -0.9 eV which are quite different than for the (111) surfaces. The -1.34-eV feature can be explained in terms of a transition from the shifted surface core level at -0.52 eV into empty states in the gap which would lie at 0.55 eV above E_F (without excitonic shifts). The absence of an analogous transition for the Si(111) surfaces shows that empty surface states on Si(111) surfaces have mostly *p* character (which makes transitions from the Si-2p-level dipole forbidden) whereas empty surface states on Si(100)-(2×1) have substantial *s* character.

Si(111)-(2×1).—The most widely accepted model is the buckled surface model,^{1,2} with alternate rows of atoms in the first layer raised and lowered and a net charge transfer to the raised atoms.

Our data are consistent with this model, i.e., the level at -0.37 eV with about a $\frac{1}{2}$ -layer intensity would correspond to the raised $\frac{1}{2}$ layer [crosshatched in Fig. 2(c)]. The lowered $\frac{1}{2}$ layer could correspond to the level at ~ -0.14 eV or at $\sim +0.16$ eV. A previous study¹² of surface core-level shifts for the 2×1 surface found a broadening consistent with our data, but attributed this to subsurface atoms by overestimating the shift for the first layer.

Si(111)-(7×7).—Various geometrical models have been proposed which can be grouped into vacancy- (or rough-) type and buckled surface- (or smooth-) type models.^{1,2,14,15} We observe $\sim \frac{1}{8}$ monolayer of atoms with a -0.7 eV core-level shift [crosshatched in Fig. 2(b)]. In a recent buckling model for Si(111)-(7×7) (Ref. 14) there exist six special up-atoms out of 49 first-layer atoms (i.e., $\sim \frac{1}{8}$ layer) which are surrounded by a particularly large number of up atoms. A recent model of the "rough" type (Ref. 15) proposes hexagonal islands of excess surface atoms. The island edge atoms should have greatly shifted core levels. Comparing the 2×1 and 7×7 surfaces as done in Ref. 14, we find that the prominent valence surface states (in normal emission) are 0.7 and 0.4 eV below E_v , respectively, thus implying significant geometry differences.

Self-consistent calculations of surface core-level shifts of semiconductors are feasible but have not yet been reported; such calculations have been reported for transition metals.¹⁶ For semiconductors, only the valence charge transfer δq between surface atoms has been calculated.⁷ The measured core-level shift δE_c can be converted into a charge transfer by using an empirical conversion factor of $\delta E_c/\delta q = 2.2$ eV/electron which has been derived from Si-2p-level shifts induced by adsorbed oxygen.¹⁷ This would imply that our observed surface core-level shifts (~ 0.2 to 0.7 eV) involve charge transfers δq of about 0.1 to 0.3 electrons/atom, in general agreement with calculations.⁷

The able assistance of J. J. Donelon, A. Marx, and the staff of the Synchrotron Radiation Center at the University of Wisconsin-Madison is acknowledged. This work was supported in part by the U. S. Air Force Office of Scientific Research, under Contract No. F49620-80-C0025.

¹For reviews, see D. R. Hamann, *Surf. Sci.* **68**, 167

- (1977); D. E. Eastman, *J. Vac. Sci. Technol.* **17**, 492 (1980).
- ²For reviews, see C. B. Duke, *CRC Crit. Rev. Solid State Mater. Sci.* **8**, 69 (1978); J. B. Pendry, *Low Energy Electron Diffraction* (Academic, London, 1974); W. Monch, *Surf. Sci.* **86**, 672 (1979).
- ³T. D. Poppendieck, T. C. Ngoc, and M. B. Webb, *Surf. Sci.* **75**, 287 (1978).
- ⁴J. A. Appelbaum and D. R. Hamann, *Surf. Sci.* **74**, 21 (1978).
- ⁵J. F. van der Veen, F. J. Himpsel, and D. E. Eastman, *Phys. Rev. Lett.* **44**, 189 (1980).
- ⁶D. E. Eastman, T.-C. Chiang, P. Heimann, and F. J. Himpsel, *Phys. Rev. Lett.* **45**, 656 (1980).
- ⁷D. J. Chadi, *Phys. Rev. Lett.* **43**, 43 (1979), and *J. Vac. Sci. Technol.* **16**, 1290 (1979).
- ⁸D. E. Eastman, J. J. Donelon, N. C. Hien, and F. J. Himpsel, *Nucl. Instrum. Methods* **172**, 327 (1980).
- ⁹G. Margaritondo and N. G. Stoffel, *Phys. Rev. Lett.* **42**, 1567 (1979).
- ¹⁰F. G. Allen and G. W. Gobeli, *Phys. Rev.* **127**, 150 (1962).
- ¹¹C. M. Garner, I. Lindau, C. Y. Su, P. Pianetta, and W. E. Spicer, *Phys. Rev. B* **19**, 3944 (1979).
- ¹²W. Eberhardt, G. Kalkoffen, C. Kunz, D. Aspnes, and M. Cardona, *Phys. Status Solidi (b)* **88**, 135 (1978).
- ¹³F. J. Himpsel and D. E. Eastman, *J. Vac. Sci. Technol.* **16**, 1297 (1979).
- ¹⁴D. J. Chadi *et al.*, *Phys. Rev. Lett.* **44**, 799 (1980).
- ¹⁵J. C. Phillips, *Phys. Rev. Lett.* **45**, 905 (1980).
- ¹⁶P. J. Feibelman and D. R. Hamann, *Solid State Commun.* **31**, 413 (1979).
- ¹⁷F. J. Grunthaner *et al.*, *Phys. Rev. Lett.* **43**, 1683 (1979).

Escape of Particles over a Dynamic Barrier

E. H. Rezayi and H. Suhl

Institute for Pure and Applied Physical Sciences, University of California, San Diego, La Jolla, California 92093

(Received 27 May 1980)

A particular example of impurity diffusion in a solid is calculated and it is noted that the usual assumptions for Brownian-motion theory are invalid in this case.

PACS numbers: 66.30.Dn, 05.40.+j

Of the multitude of processes in physics and chemistry that involve activated escape of a "particle" over a barrier (chemical reactions, dynamics of certain spin-glass models, diffusion, superionic conductors, etc.) only those are adequately understood that involve a clear separation of time scales of "particle" and "heat-bath" motion. The effect of the heat bath is then represented by a friction coefficient. According to Kramers,¹ when this friction coefficient lies in a certain range, the so-called absolute-rate theory (ART) applies, and in this range, the escape rate is practically independent of the value of the friction, i.e., independent of the dynamics of the particle-bath interaction. Purely statistical arguments then give the escape rate. The term "particle," in general, refers to the representative point in the multidimensional configuration space of a many-particle system. Vinyard's² theory of impurity diffusion in a crystalline solid is an example of ART (at each step of the diffusion process the crystal configuration is assumed entirely relaxed). The rate is then the forward current per particle over the saddle point of the energy hypersurface. However, the rate of motion of the host and impurity atoms are not sig-

nificantly different; thus the preconditions for Kramers' theory in general and ART in particular are not met, at least not insofar as the host acts as heat bath. Nor will they be met in the important case of a chemical reaction on the surface of an insulator. It is to be emphasized that there are at present no reliable theories in the absence of the particular separation of time scales mentioned above. However, in one particular case, namely that of an impurity bound in a lattice in such a way so as to give rise to a well-defined local mode, it is possible to calculate an approximate diffusion rate of the impurity without Langevin-Fokker-Planck assumptions.

Escape over the barrier here corresponds to mode instability and the escape rate is the average number of times per second that instability conditions are met. The anharmonicity causes instability in three ways: (i) Impinging phonons occasionally excite the mode to an amplitude it cannot stably sustain. (ii) The incident phonons modulate the effective local mode frequency, occasionally turning it imaginary. (iii) Parametric excitation by incident phonons.

Processes (ii) and (iii) combined dominate the rate. They are related to an effect proposed by